THE JOURNAL OF BIOLOGICAL CHEMISTRY VOL. 288, NO. 3, pp. 1871–1882, January 18, 2013
© 2013 by The American Society for Biochemistry and Molecular Biology, Inc. Published in the U.S.A.

Arabidopsis Calmodulin-binding Protein IQ67-Domain 1 Localizes to Microtubules and Interacts with Kinesin Light Chain-related Protein-1*[S]

Received for publication, June 29, 2012, and in revised form, November 29, 2012 Published, JBC Papers in Press, November 30, 2012, DOI 10.1074/jbc.M112.396200

Katharina Bürstenbinder[‡1], Tatyana Savchenko[§1,2], Jens Müller[‡1], Aaron W. Adamson[§3], Gina Stamm[‡], Raymond Kwong[§4], Brandon J. Zipp[§5], Dhurvas Chandrasekaran Dinesh[‡], and Steffen Abel[‡§¶6]

From the [‡]Department of Molecular Signal Processing, Leibniz Institute of Plant Biochemistry, D-06120 Halle, Germany, the [§]Department of Plant Sciences, University of California, Davis, California 95616, and the [¶]Institute of Biochemistry and Biotechnology, Martin Luther University Halle-Wittenberg, D-06120 Halle, Germany

Background: Plant-specific *IQD* genes encode putative CaM targets of unknown functions.
Results: IQD1 interacts with KLCR1, binds to *Arabidopsis* CaM/CMLs, and localizes to microtubules.
Conclusion: IQD1 may act as a scaffold protein recruiting cargo to kinesin motors for directional transport along microtubules.
Significance: This work provides novel insight into IQD function and a framework to study plant kinesin regulation.

Calcium (Ca^{2+}) is a key second messenger in eukaryotes and regulates diverse cellular processes, most notably via calmodulin (CaM). In *Arabidopsis thaliana*, IQD1 (IQ67 domain 1) is the founding member of the IQD family of putative CaM targets. The 33 predicted IQD proteins share a conserved domain of 67 amino acids that is characterized by a unique arrangement of multiple CaM recruitment motifs, including so-called IQ motifs. Whereas IQD1 has been implicated in the regulation of defense metabolism, the biochemical functions of IQD proteins remain to be elucidated. In this study we show that IQD1 binds to multiple *Arabidopsis* CaM and CaM-like (CML) proteins *in vitro* and in yeast two-hybrid interaction assays. CaM overlay assays revealed moderate affinity of IQD1 to CaM2 ($K_d \sim 0.6\ \mu M$). Deletion mapping of IQD1 demonstrated the importance of the IQ67 domain for CaM2 binding *in vitro*, which is corroborated by interaction of the shortest IQD member, IQD20, with *Arabidopsis* CaM/CMLs in yeast. A genetic screen of a cDNA library identified *Arabidopsis* kinesin light chain-related protein-1 (KLCR1) as an IQD1 interactor. The subcellular localization of GFP-tagged IQD1 proteins to microtubules and the cell nucleus in transiently and stably transformed plant tissues (tobacco leaves and *Arabidopsis* seedlings) suggests direct interaction of IQD1 and KLCR1 *in planta* that is supported by GFP∼IQD1-dependent recruitment of RFP∼KLCR1 and RFP∼CaM2 to microtubules. Collectively, the prospect arises that IQD1 and related proteins provide Ca^{2+}/CaM-regulated scaffolds for facilitating cellular transport of specific cargo along microtubular tracks via kinesin motor proteins.

In plants, intracellular Ca^{2+} plays a pivotal role as a second messenger for the regulation of numerous developmental processes and responses to a myriad of abiotic cues and biotic challenges (1–3). Typically, Ca^{2+} signaling pathways comprise three stages. Stimulus-specific and dynamic fluctuations of cytosolic Ca^{2+} concentration, characterized by amplitude, frequency, and spatial distribution, are generated during the initial phase by interplay of voltage- and ligand-activated Ca^{2+}-permeable channels (influx) and Ca^{2+}-ATPases/antiporters (efflux) to restore resting cytosolic Ca^{2+} levels. The resulting Ca^{2+} signatures are decoded by Ca^{2+}-sensor proteins that undergo conformational changes upon Ca^{2+} binding followed by dynamic interactions with target proteins to regulate downstream responses during the final stage of the transduction process (1–3).

About 250 Ca^{2+} sensor proteins have been identified in the reference plant *Arabidopsis thaliana*, which monitor Ca^{2+} fluctuations via their helix-loop-helix EF hand motifs and can be grouped into Ca^{2+} sensor responders or Ca^{2+} sensor relays (4, 5). The former are bifunctional proteins capable of directly transducing the Ca^{2+} signal via their intrinsic catalytic activity. For example, Ca^{2+}-dependent protein kinases, a family of 34 members in *Arabidopsis*, couple Ca^{2+} binding motifs with a kinase domain to catalyze Ca^{2+}-triggered phosphorylation of target proteins (6). In contrast, the more widespread Ca^{2+} sen-

* This work was supported by the National Research Initiative of the United States Department of Agriculture Cooperative State Research Education and Extension Service Grant 2005-02507 (to S. A.), by a predoctoral fellowship from the Deutsche Forschungsgemeinschaft (GRK1026; to D. C. D.), and by core funding to the Leibniz-Institute of Plant Biochemistry from the state of Saxony-Anhalt and the Federal Republic of Germany.
[S] This article contains supplemental Figs. S1–S5.
[1] These authors contributed equally to this work.
[2] Present address: Institute of Basic Biological Problems, Russian Academy of Sciences, Moscow Region, Pushchino, 142290 Russia.
[3] Present address: Dept. of Population Sciences, 1500 East Duarte Rd., City of Hope, Duarte, CA 91010.
[4] Present address: Siemens Healthcare Diagnostics, 2040 Enterprise Blvd., Sacramento, CA 95691.
[5] Present address: Biochemistry, Molecular, Cellular and Developmental Biology Graduate Group, University of California-Davis, One Shields Ave., Davis, CA 95616.
[6] To whom correspondence should be addressed: Dept. of Molecular Signal Processing, Leibniz Institute of Plant Biochemistry, Weinberg 3, D-06120 Halle, Germany. Tel.: 49-345-5582-1200; Fax: 49-345-5582-1209; E-mail: sabel@ipb-halle.de.

sor relays a lack catalytic activity, such as calmodulins (CaMs),[7] CaM-like proteins (CMLs), and calcineurin B-like proteins. The Ca^{2+} sensor relays undergo conformational changes upon Ca^{2+} binding and transduces the signal via interaction with terminal Ca^{2+} responders, thereby modulating the biochemical activities of these target proteins and establishing a large number of cellular processes and subsequent plant responses (1–3). In *Arabidopsis*, 10 calcineurin B-like protein sensor proteins interact specifically in a Ca^{2+}-dependent fashion with a single family of 26 SNF1-like Ser/Thr kinases, known as calcineurin B-like protein-interacting protein kinases (CIPKs). Current data indicate that calcineurin B-like protein-CIPK interaction networks provide a signaling module for integrating plant responses to an array of environmental stimuli (7, 8). On the other hand, CaMs and CMLs, encoded by 7 CaM and 50 CML genes in *Arabidopsis*, regulate a broad range of structurally diverse Ca^{2+} responders that are predicted to exceed 700 target proteins (9, 10). These include, among other functional categories, proteins implicated in generating Ca^{2+} signatures, enzymes in signaling and metabolic pathways, and transcriptional regulators (11, 12). The CaM-interacting domains of target proteins usually consist of a short basic amphiphilic helix (12–30 residues). Three consensus CaM recruitment motifs are currently known, although not all functionally characterized CaM binding domains contain these specific motifs: the IQ motif mediating Ca^{2+}-independent CaM retention and two related motifs, termed 1-5-10 and 1-8-14, facilitating Ca^{2+}-dependent CaM interaction (13–15).

We previously identified a novel class of putative CaM target proteins in *A. thaliana* that we called the IQD family (16, 17). The common feature of its 33 members is the presence of a plant-specific, central domain of 67 conserved amino acid residues (referred to as the IQ67 domain), which is defined by a unique and repetitive arrangement of the three consensus CaM recruitment motifs (1–3 copies each). IQD proteins are structurally diverse with respect to computed molecular mass (12–87 kDa) but are relatively uniform at the physicochemical level, sharing some properties reminiscent of RNA binding proteins, such as a basic isoelectric point (pI ~ 10.3) and a high content of Arg/Lys (~17%) and Ser (~12%) residues (17). Another hallmark of the *Arabidopsis* IQD family is a high fraction of homeologous gene pairs (~45% of the paralogous gene set), which is characteristic of protein families with conserved functions in regulatory multiprotein complexes (17). However, given the large size of the extant plant *IQD* gene families, which originated during the early evolution of land plants and their likely conserved functions (17), surprisingly little is known about the biological roles of IQD proteins.

The first described *IQD* gene was functionally identified in a screen for *Arabidopsis* mutants with altered production of glucosinolates (16), a class of secondary metabolites in crucifers whose degradation products possess profound biological activities ranging from plant defense to cancer prevention in humans (18, 19). IQD1 binds to vertebrate CaM in a Ca^{2+}-dependent fashion, which is also true for IQD20, the smallest member of the *Arabidopsis* IQD family, consisting only of the IQ67 domain at its C terminus and a short N-terminal extension (16, 17). An IQD1~GFP fusion protein localizes to the cell nucleus, and histochemical analysis of $IQD1_{Pro}$::*GUS* lines reveals patterns of reporter gene expression consistent with tissue-specific glucosinolate biosynthesis. Overexpression of *IQD1* in *Arabidopsis* stimulates glucosinolate accumulation and defense against herbivores. Because *IQD1* expression is induced by mechanical stimuli, IQD1 was proposed to act as a nuclear factor that integrates intracellular Ca^{2+} signals to regulate defense metabolism in response to biotic challenge (16).

Besides IQD1, another member of the *Arabidopsis* family, IQD22, has been implicated as a negative regulator of the response to the plant hormone gibberellin (20), and a role for IQD12 from tomato (*Solanum lycopersicum*) has recently been revealed (21, 22). The *sun* quantitative trait locus is associated with tomato fruit shape and causes long, atypically formed fruits when compared with the wild ancestor. A genetic approach identified *IQD12* to be a major gene responsible for fruit shape variation and showed that its high expression level, caused by retrotransposon-mediated *IQD12* duplication, leads to extremely elongated tomato fruits via altered cell division patterns (21, 22). Whereas first biological processes regulated by IQD proteins are beginning to emerge that include aspects of plant development or defense response, their molecular functions and underlying signaling pathways remain to be elucidated.

Here, we expand our studies on *Arabidopsis* IQD1 and describe its direct interaction with a select set of *Arabidopsis* CaM/CMLs. Using a genetic yeast two-hybrid interaction screen, we identified kinesin light chain-related-1 (KLCR1) as an IQD1 binding protein in *Arabidopsis*, which prompted us to reinvestigate the subcellular localization of IQD1 at high resolution. Interestingly, our data demonstrate that IQD1 localizes not only to the cell nucleus but also associates with the microtubular network to which IQD1 recruits KCLR1 as well as CaM2. For the first time our work provides insight into the biochemical function of IQD1 and related proteins as putative Ca^{2+}-CaM-regulated scaffold proteins, which may facilitate cellular transport of cargo complexes via microtubule-associated kinesin motor proteins.

EXPERIMENTAL PROCEDURES

Production of Recombinant Proteins—The bacterial vector for expression of recombinant IQD1 fused to an N-terminal T7 epitope tag was previously described (16). Similarly, full-length cDNA fragments encoding the predicted *Arabidopsis* IQD20 and IQD33 proteins were generated by RT-PCR using gene-specific primers and mobilized into the pET21a(+) vector (BamHI/EcoRI), which provides the N-terminal T7 tag (Novagen, Madison, WI). To allow for production of recombinant proteins with two epitope tags (N-terminal T7 tag, C-terminal His_6 tag), full-length IQD1 and partial cDNAs encoding truncated IQD1 polypeptides were generated by PCR and mobilized into the pET21a(+) vector (EcoRI/HindIII). Production of

[7] The abbreviations used are: CaM, calmodulin; CML, CaM-like protein; IQD1, IQ67 domain 1; KLCR1, kinesin light chain-related-1; SD, synthetic dropout; X-gal, β-galactosidase substrate 5-bromo-4-chloro-indolyl-β-D-galactopyranoside; BD, binding domain; AD, activation domain; KLC, kinesin light chain; KLCR, KLC-related; KLCR1, KLC-related protein-1; mRFP, monomeric red fluorescent protein (RFP).

recombinant *Arabidopsis* CaM1 (identical with CaM4), CaM2 (identical with CaM3 and CaM5), CML8, and CML9 fused to the C-terminal Strep-tag II was supported by pASK-IBA3 bacterial vectors (Genosys Biotechnologies, Inc., The Woodlands, TX), which were obtained from C. Köhler (23). The authenticity of all cloned cDNA fragments was verified by DNA sequencing. Plasmids were transformed into *Escherichia coli* BL21a(pLysS) DE3 cells (Novagen) for protein expression and purification using standard protocols. Expression of recombinant proteins was induced by 1 mM isopropyl β-D-thiogalactopyranoside for at least 4 h at 37 °C. Bacterial cells were lysed by sonication in buffer A (25 mM Tris-HCl, pH 7.5, 50 mM NaCl, 0.1% Triton X-100) for most experiments or in buffer B (10 mM Tris-HCl, pH 7.6, 2.5 mM $MgCl_2$, 0.5% Triton X-100) for nucleic acid binding experiments. Both buffers contained 1 tablet of complete EDTA-free protease inhibitor mixture (Roche Applied Science) per 50 ml volume. Bacterial lysates were cleared by centrifugation at 14,000 rpm for 30 min at 4 °C. The supernatants were used for SDS-PAGE, protein purification, immunoblot analysis, and *in vitro* interaction assays.

Calmodulin Pulldown Assays—Cell extracts of bacteria expressing C-terminal Strep-tag II fusions of *Arabidopsis* CaM1, CaM2, CML8, or CML9 were incubated with Strep-Tactin beads according to the manufacturer's protocol (Genosys Biotechnologies) to allow for binding of recombinant CaM/CML proteins. Aliquots of Strep-Tactin beads with bound CaM/CMLs (60 μl) were washed with buffer A containing 1 mM $CaCl_2$ or 5 mM EGTA. Bacterial lysates expressing T7-tagged IQD1 (400 μl) were added to the prewashed beads in the presence of 1 mM $CaCl_2$ or 5 mM EGTA. The suspensions were rotated at room temperature for 30 min. After incubation, the beads were washed 4 times with 1 ml of buffer A containing 1 mM $CaCl_2$ or 5 mM EGTA. The bound proteins were eluted by boiling the bead pellets for 2 min in 50 μl of SDS sample buffer. Proteins were resolved on 10% (w/v) SDS- polyacrylamide gels (24) and transferred to nitrocellulose membranes (Pierce). Cosedimentation of T7-tagged IQD1 was detected by enhanced chemiluminescence using a horseradish peroxidase (HRP)-conjugated T7-Tag monoclonal antibody (Novagen) as previously described (16).

Calmodulin Overlay Assays—The coding region of *Arabidopsis CaM2* was cloned into vector pENTR1A (Invitrogen) using BamHI and XhoI restriction sites. The resulting entry vector was used to mobilize the *CaM2* cDNA insert by LR recombination (according to the manufacturer's protocol) into vector pEXP1-DEST (Invitrogen) to facilitate *in vitro* synthesis of CaM2 containing a His_6-tag, the Xpress epitope tag, and the enterokinase recognition site. The cell-free protein synthesis system Expressway Cell-Free *E. coli* Expression System (Invitrogen) and [^{35}S]methionine (Met) (Amersham Biosciences) were used for the production of recombinant [^{35}S]Met-labeled CaM2 according to the manufacturer's protocol. The radiolabeled CaM2 was purified by Ni-NTA affinity chromatography (Qiagen, Valencia, CA) under native conditions and digested *in situ* with enterokinase EKMax™ (Invitrogen) overnight at 37 °C. The released CaM2 was collected in the flow-through fraction. The concentration of the purified protein was determined by measuring the absorbance at 280 nm using extinction coefficient values calculated by the ExPASy ProtPARAM tool (13,980 M^{-1} cm^{-1} for the CaM2 fusion after enterokinase cleavage). Purified CaM2 was used as a probe after determination of its concentration and specific radioactivity (about 0.5×10^6 cpm/μg). Expressed T7- and His_6-tagged full-length IQD proteins and truncated IQD1 polypeptides were purified by Ni-NTA affinity chromatography under native conditions (according to the manufacturer's protocol). The proteins (0.5 μg) were separated by SDS-PAGE (12% gels) and transferred to nitrocellulose membranes. The membranes were blocked overnight with 5% BSA in TBST buffer (50 mM Tris-HCl, pH 7.4, 150 mM NaCl, 0.1% Tween 20) and subsequently overlaid with 2 mM [^{35}S]Met-labeled CaM2 in the same buffer containing 1 mM $CaCl_2$ or 5 mM EGTA. The membranes were washed 4 times for 15 min in the respective buffers without probe. Bound CaM2 was detected by phosphorimaging analysis (GE Healthcare).

For determining saturation curves of CaM2 binding, full-length T7-IQD1-His_6 recombinant protein was purified by Ni-NTA chromatography under native conditions and spotted on nitrocellulose membrane discs (100 pmol) that were sequentially incubated in blocking solution (see above) for 1 h at room temperature followed by incubation in blocking solution containing different concentrations of [^{35}S]Met-labeled CaM2 in the presence of 1 mM $CaCl_2$ or 5 mM EGTA (2 h at room temperature). After washing in TBST buffer without radiolabeled CaM2, the amount of bound CaM2 was measured by liquid scintillation counting. Not more than 0.1% of added [^{35}S]Met-labeled CaM2 remained at the membrane at any condition. Specific CaM2 binding was calculated as the difference between total binding and nonspecific binding (filter discs without recombinant IQD1 protein). The K_d value was determined by Scatchard plot analysis.

Yeast Two-hybrid Assays—For yeast two-hybrid interaction assays, the coding sequences of IQD1 and IQD20 were amplified by PCR and cloned into the bait pGBT9 vector (SpeI/EcoRI) to create plasmids encoding IQD protein fusions with the Gal4 DNA binding domain (23). Plasmids encoding fusions of *Arabidopsis* CaMs and CMLs with the Gal4 activation domain were obtained either from C. Köhler (23) (pGAD-CaM1, pGAD-CaM2, pGAD-CML8, pGAD-CML9) or were constructed by PCR and insert mobilization into the prey pGAD424 vector for CaM6 (XhoI/EcoRI), CML5 (XhoI/EcoRI), CML11 (BamHI/XhoI), CML13 (XhoI/EcoRI), CML17 (BamHI/EcoRI), CML19 (XhoI/EcoRI), CML27 (XhoI/NotI), CML36 (XhoI/EcoRI), and CML49 (XhoI/EcoRI). Plasmid templates for *Arabidopsis* CaMs and CMLs cDNAs were obtained from the Arabidopsis Biological Resource Center (Columbus, OH). Full-length cDNAs of IQD1 and IQD20 were also inserted into pGAD424 (BamHI/EcoRI) to test for *in vivo* homodimerization. All plasmid constructs were verified by DNA sequencing. Plasmid pGAD-CNGC2 served as a positive control for CaM interaction and was provided by C. Köhler (23). The bait and prey vectors to be tested for interaction of the fusion proteins were co-transformed into yeast (*Saccharomyces cerevisiae*) strain HF7c using the standard lithium acetate method (25). Protein-protein interactions were scored and quantified by the ability to activate two reporter genes under control of the *GAL4* promoter: *HIS3* and *lacZ*. The *HIS3*

reporter activity was monitored by testing transformants on synthetic dropout (SD) medium lacking histidine (His). Yeast colonies selected for the presence of the bait and prey plasmids were grown in liquid SD medium (−Leu-Trp) to an optical density of 1 A_{600}. Serial 10-fold dilutions (10 μl) were spotted on growth permissive (−Leu-Trp) and growth restrictive (−Leu-Trp-His) SD agar plates. *LacZ* reporter gene expression (β-galactosidase activity) was determined using *O*-nitrophenyl-β-D-galactopyranoside as a substrate (25), and the galactosidase activity was calculated as Miller units: $A_{420} \times 1000/A_{600} \times$ assay time (min) $\times$ assay volume (ml).

cDNA Library Construction—An *A. thaliana* (ecotype Columbia) flower cDNA library was constructed using the BD-Matchmaker Library Construction and Screening Kit (Clontech, Mountain View, CA). Poly(A)$^+$ RNA (100 ng) prepared from flower tissues was used for cDNA synthesis according to the manufacturer's instruction. First strand cDNA was amplified by long distance PCR using the BD Advantage 2 PCR kit (Clontech). The purified cDNA was then fused to the GAL4 activation domain of the bait pGADT7-Rec (Clontech) expression vector by recombination in AH109 yeast strain, which yielded more than four million original transformants.

Yeast Two-hybrid Screening—The yeast two-hybrid cDNA library screening was performed using the BD Matchmaker Two-hybrid System (BD Biosciences). Full-length cDNA of IQD1 was amplified by PCR and cloned into the GAL4 DNA binding domain of pGBKT7 (BD Biosciences), generating bait plasmid pGBKT7-IQD1, which was sequenced to ensure fidelity of the construct. The bait construct was introduced into yeast strain Y187 using the lithium acetate transformation method (BD Biosciences Yeast Protocols Handbook). Screens were carried out by mating according to the manufacturer's instructions (Clontech). Briefly, an overnight culture of strain Y187 expressing pGBKT7-IQD1 was mixed with strain AH109, harboring the flower cDNA library, for 24 h in rich medium at 30 °C in a shaker at low rotation (30–50 rpm). The mixed yeast culture (diploid cells) was then plated on restrictive SD medium lacking Trp, Leu, His, and adenine (Ade). Positive colonies appearing within 5 days of plating (presumably caused by activation of the *HIS3* and *ADE2* reporter genes) were subsequently streaked on restrictive SD medium and tested for *lacZ* expression by a liquid ONPG β-galactosidase assay (BD Biosciences Yeast Protocols Handbook) to estimate the strength of interactions. Clones generating Miller units >1.0 were regarded as candidates. After the confirmation of the growth phenotype and *lacZ* expression, plasmid DNA was isolated from yeast cells and transformed into *E. coli* strain DH5α by electroporation. Because the isolated DNA is a mixture of both plasmids (the bait and prey library clone), the transformed *E. coli* were plated on LB medium containing ampicillin to select for the AD-cDNA library plasmid only. The cDNA inserts were amplified using the BD Matchmaker AD LD-Insert Screening Amplimer Set (Clontech) and the BD Advantage 2 PCR kit (Clontech) to analyze the number of AD library plasmids they contain. Each positive clone generated only one PCR product (one type of AD-cDNA library plasmid). The plasmid was then sequenced, and the cDNA insert was subjected to BLAST analysis of the NCBI database. To independently confirm interaction in the yeast two-hybrid system, the yeast strains Y187 and AH109 were transformed with the respective constructs, mated, and tested for growth on restrictive (−Trp-Leu-His-Ade) SD medium in the presence of 20 μg/ml of the chromogenic β-galactosidase substrate 5-bromo-4-chloro-indolyl-β-D-galactopyranoside (X-Gal).

Subcellular Localization Studies—The coding sequences of IQD1, KLCR1, and CaM2 were amplified in combination with a high fidelity DNA polymerase and subsequently inserted into pENTR/D-TOPO plasmid via directional TOPO cloning (Invitrogen) to generate IQD1-, KLCR1-, and CaM2-pENTR/D-TOPO vectors. A derivative plasmid lacking the IQD1 stop codon, IQD1*-pENTR/D-TOPO, was generated via site-directed mutagenesis (Stratagene, La Jolla, CA) according to the manufacturer's protocol. The fidelity of the inserts was verified by DNA sequencing. To study the subcellular localization of GFP- or RFP-tagged fusion proteins, IQD1-, KLCR1-, or CaM2-pENTR/D-TOPO and the IQD1*-pENTR/D-TOPO entry plasmids were recombined in LR clonase reactions with the Gateway-compatible binary destination vectors pB7WG2, pB7WGF2, or pB7FWG2 (26) to generate *CaMV* $35S_{Pro}$::*IQD1*, $35S_{Pro}$::*GFP~IQD1*, $35S_{Pro}$::*GFP~KLCR1*, and $35S_{Pro}$::*IQD1~GFP* plasmid constructs. For generation of $35S_{Pro}$::*mRFP~CaM2* and $35S_{Pro}$::*mRFP~KLCR1* constructs, the pGWB455 destination vector was used (27).

Agrobacterium-mediated transient transformation of tobacco leaves (*Nicotiana benthamiana*) was conducted as described (28). After infiltration (1–3 days), samples were collected, and GFP fluorescence was visualized on a Zeiss LSM 710 confocal laser scanning microscope. All images were obtained using a 40× water-immersion objective. The excitation wavelength was 488 nm; emission was detected between 493 and 580 nm. For treatments, a 50 μM aqueous oryzalin solution (Sigma) was prepared from a 200 mM stock dissolved in DMSO, and tobacco leaves were infiltrated 1.5 h before microscopic analysis. For co-localization studies, tobacco leaves were co-infiltrated with the indicated plasmids, and fluorescence was visualized on a Zeiss LSM 700. All images were obtained using the sequential mode to prevent false positive signals. A 488-nm (GFP) and a 555-nm (RFP) diode laser were used for excitation; emission was detected using a short pass filter (492–555 nm) and a long pass filter (582–700 nm) for GFP and RFP, respectively. Transgenic *Arabidopsis* plants were generated by *Agrobacterium*-mediated transformation. T_2 lines showing a segregation ratio of 3:1 for resistance to Basta® were selected for subsequent microscopic analysis (29). Oryzalin treatments (5 μM) on *Arabidopsis* plants were done for 60 min.

Whole-mount immunolocalization experiments were performed as previously described (30) using a rat anti-α-tubulin antibody (MCA78G) (AbD Serotec, Düsseldorf, Germany). After successive washings, samples were incubated with a red fluorescent rabbit anti-rat (SAB4600122) and a monoclonal green fluorescent mouse anti-GFP antibody (SAB4600051) (Sigma). Microscopy was conducted as described for co-localization studies on transiently transformed tobacco leaves.

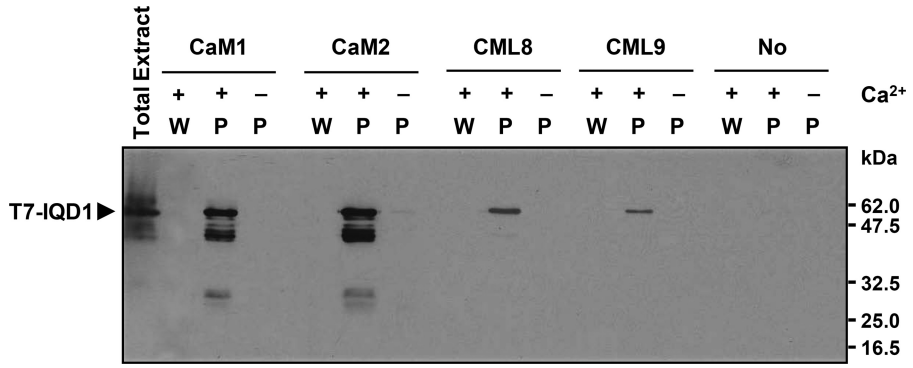

FIGURE 1. ***Arabidopsis* IQD1 interacts with *Arabidopsis* CaM/CMLs *in vitro*.** Strep-Tactin beads loaded with Strep-tagged calmodulins (CaM1, CaM2) or calmodulin-like proteins (CML8, CML9) were incubated with bacterial extracts expressing full-length T7-tagged IQD1 at room temperature in the presence of 1 mM $CaCl_2$ (+) or 5 mM EGTA (−). Proteins of the total bacterial extract (*leftmost lane*), of the last wash (*W*), and of the entire pellet (beads) fraction (*P*) were resolved by SDS-PAGE, transferred to a membrane, and probed with an HRP-conjugated T7-Tag monoclonal antibody, which detected the full-length T7-IQD1 protein (*arrowhead*) and several fragments. The *rightmost three lanes* demonstrate that T7-IQD1 does not bind to the Strep-Tactin matrix in the absence (*No*) of CaMs or CMLs.

RESULTS

IQD1 and Arabidopsis CaM/CMLs Interact in Vitro—We previously demonstrated Ca^{2+}-dependent interaction of T7 epitope-tagged *Arabidopsis* IQD1 with bovine CaM (16). Here we extended these studies to include several *Arabidopsis* CaMs and CML proteins (Fig. 1). In *Arabidopsis*, 7 and 50 genes code for canonical CaMs and CML proteins, respectively. The 7 distinct CaM loci encode 4 CaM isoforms (CaM1/4, CaM2/3/5, CaM6, CaM7), which differ by 1–4 residues and share at least 89% identity to conserved vertebrate CaMs (10). We performed *in vitro* pulldown assays with T7-IQD1 and two *Arabidopsis* CaM isoforms, CaM1 and CaM2, as well as with two CML proteins, CML8 and CML9. We included CML8 and CML9 because both proteins differ considerably from conventional CaMs (<75% sequence identity). The Strep-tagged CaMs and CMLs were expressed in *E. coli* and purified by affinity chromatography on Strep-Tactin-Sepharose beads. After co-incubation of Strep-tagged CaMs or CMLs (bead-immobilized) and T7-epitope tagged IQD1 (bacterial extracts) in the presence of 1 mM $CaCl_2$ or 5 mM EGTA, the Strep-Tactin-Sepharose beads were repeatedly washed. Bound proteins were eluted by boiling in SDS sample loading buffer. Proteins of all fractions were separated by SDS-PAGE, transferred to a membrane, and probed with T7-tag monoclonal antibody to detect T7-IQD1 fusion protein. As shown in Fig. 1, full-length T7-IQD1 co-sedimented with all tested CaMs and CMLs only in the presence of Ca^{2+}, and binding was abolished when EGTA was added to the buffer. In summary, the data confirm our previous results with bovine CaM (16) and demonstrate the capacity of *Arabidopsis* IQD1 to interact in a Ca^{2+}-dependent manner with various *Arabidopsis* CaMs and CMLs *in vitro*.

The IQ67 Domain Mediates CaM Binding in Vitro—In a first approach to experimentally delineate the CaM binding region of IQD proteins, we took advantage of the structural diversity of the IQD family in *Arabidopsis*. Whereas IQD20, the smallest IQD member (103 amino acid residues), comprises the IQ67 domain at its C terminus and a short N-terminal extension of 35 amino acid residues, the IQD33 protein (442 amino acid residues) misses 51 residues of its centrally positioned IQ67 motif, which was likely caused by exon loss (17). We employed CaM overlay assays to compare the ability of IQD1, IQD20, and IQD33 to interact with CaM2 in a Ca^{2+}-dependent manner. The T7-tagged IQD proteins were expressed in bacteria, and total protein extracts were separated by SDS-PAGE, transferred to nitrocellulose membranes, renatured, and probed with radiolabeled CaM2, which was prepared by *in vitro* transcription/translation in the presence of [^{35}S]Met followed by affinity chromatography purification on Ni-NTA and proteolytic removal of the His_6 epitope tag. As a positive control, we used bacterial lysates expressing *Arabidopsis* CNGC1 (23), which did bind to [^{35}S]Met-labeled CaM2 in the presence of calcium (1 mM $CaCl_2$) but not in its absence (5 mM EGTA) (supplemental Fig. S1). We also observed an interaction of the CaM2 probe with IQD1 and IQD20, but not with IQD33. In contrast to the pulldown assays (Fig. 1), CaM binding was only detected in the absence of Ca^{2+} (supplemental Fig. S1), which is not an uncommon observation for IQ motif-containing proteins (31, 32). In conclusion, our data point to the importance of the IQ67 domain for mediating CaM/CML interaction.

In a second approach to map the CaM interaction domain of IQD proteins, we generated a series of overlapping N- and C-terminal deletions of IQD1, each tagged with T7 and His_6 epitopes (T7-IQD1-His_6) that we tested for CaM binding in overlay assays (Fig. 2*A*). Full-length IQD1 and truncated IQD1 polypeptides were affinity-purified by Ni-NTA chromatography, separated by SDS-PAGE, transferred to nitrocellulose membranes, renatured, and probed with [^{35}S]Met-labeled CaM2 as above. Protein loading was assessed by T7 epitope detection (Fig. 2*B*). As expected, CaM2 binding was only observed for IQD1 polypeptides comprising the IQ67 domain, which further supports a role of this domain for recruiting CaM (Fig. 2, *C* and *D*). Using full-length IQD1 protein, we determined by CaM overlay assays and Scatchard plot analysis the apparent dissociation constant of the interaction between IQD1 and CaM2 (Fig. 3). The calculated value ($K_d \sim 0.6\ \mu$M) indicates a relatively low affinity of IQD1 for CaM2 under the *in vitro* assay conditions used.

IQD1and IQD20 Interact with CaM/CMLs in Yeast—We previously showed Ca^{2+}-dependent interaction of T7-IQD1 and T7-IQD20 with bovine CaM (16, 17). To validate *in vivo* the

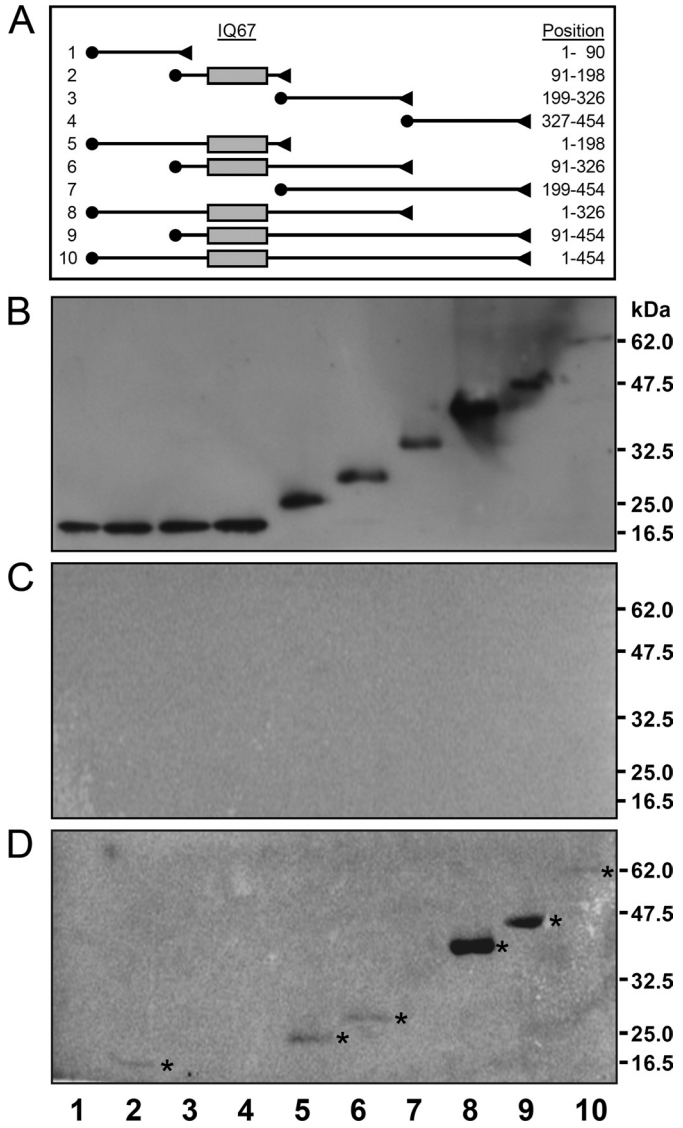

FIGURE 2. **Mapping of the CaM binding domain in IQD1.** Full-length epitope-tagged T7-IQD1-His_6 and nine derived truncated IQD1 polypeptides were purified by affinity chromatography on Ni-NTA, separated by SDS-PAGE, transferred to a membrane, and probed with [^{35}S]Met-labeled CaM2 in the presence of 1 mM $CaCl_2$ or 5 mM EGTA as described under "Experimental Procedures." *A*, shown is a map of the 10 epitope-tagged IQD1constructs. The N-terminal T7 tag and the C-terminal His_6 tag are indicated by *solid circles* and *triangles*, respectively. The *gray box* denotes the IQ67 domain, and the length of each IQD1-derived polypeptide is given on the *right* (position of amino acid residues). *B*, shown is immunodetection of SDS-PAGE, resolved Ni-NTA-affinity-purified IQD1 polypeptides with an HRP-conjugated T7-tag monoclonal antibody. *C* and *D*, overlay assays with [^{35}S]Met-labeled CaM2 in the presence of 1 mM $CaCl_2$ (*C*) or 5 mM EGTA (*D*) is shown. Note only IQD1-derived polypeptides containing the IQ67 domain bind to *Arabidopsis* CaM2 (*asterisks* in *D*).

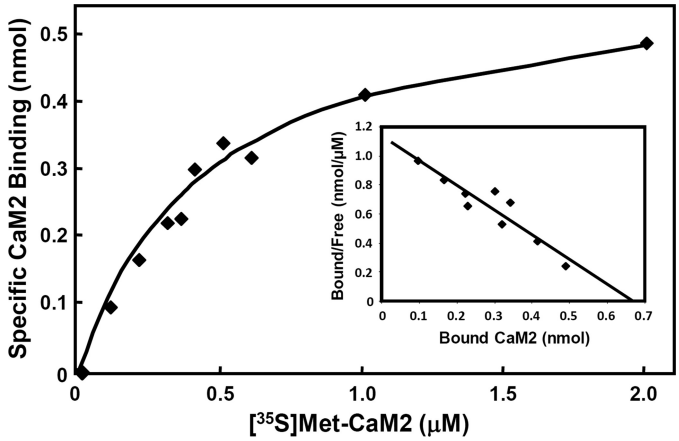

FIGURE 3. **Binding of [^{35}S]Met-labeled CaM2 to IQD1.** [^{35}S]Met-labeled *Arabidopsis* CaM2 and affinity-purified T7- IQD1-His_6 protein were prepared as described under "Experimental Procedures." The recombinant IQD1 (1 μmol) was immobilized on a nitrocellulose membrane and incubated with increasing concentrations of [^{35}S]Met-labeled CaM2. The membranes were washed to remove unbound CaM2, and bound radioactivity was measured in a liquid scintillation counter. Each measurement was the average of three repeats. The specifically IQD1-bound [^{35}S]Met-labeled CaM2 (*y* axis) at the indicated total concentrations of the [^{35}S]Met-labeled CaM2 ligand (*x* axis) was graphed. The *inset* shows the Scatchard plots for CaM2 binding. The bound [^{35}S]Met-labeled CaM2 was plotted against the ratio of bound to free CaM2.

observed *in vitro* interactions of IQD1 and IQD20 with CaM, we performed yeast two-hybrid interaction assays. Both IQD proteins were fused to the Gal4 DNA binding domain (Gal4BD (BD)) or Gal4 activation domain (Gal4AD (AD)). We selected 13 CaM/CML proteins representing the nine groups of the *Arabidopsis* CaM/CML family (33) for construction of Gal4AD-CaM/CML prey vectors. A CNGC2 bait vector (Gal4DB-CNGC2) was used as a positive control for CaM interaction in yeast (23). The respective bait and prey vectors were co-transformed into the yeast reporter strain HF7c harboring two reporter genes integrated into the chromosome, *His3* and *LacZ*. The *His3* reporter activity was assayed by testing the growth of transformants on SD medium lacking His. *LacZ* reporter gene expression was monitored by a quantitative enzyme assay of β-galactosidase activity. As shown in Fig. 4, none of the negative controls was able to grow on restrictive (−Leu-Trp-His) SD medium (*i.e.* single transformations with BD-IQD1 and BD-IQD20 or AD-CaM1, AD-CaM2, AD-CaM7, AD-CML11, and AD-CML13), whereas the positive control (co-transformation with AD-CaM1/BD-CNGC2) revealed robust growth and expression of β-galactosidase activity (15.1 Miller units), which was similar to published results (23). Furthermore, there was no evidence for homotypic interaction of IQD1 or IQD20 (co-transformation with BD-IQD1/AD-IQD1 or BD-IQD20/AD-IQD20). When compared with the positive control, yeast cells transformed with plasmids encoding BD-IQD1 and AD-CaMs (CaM1, CaM2, CaM7) showed only weak growth on SD medium lacking His and low expression of β-galactosidase activity (~0.3 Miller units). However, co-transformation with BD-IQD1 and each of the 10 different AD-CML constructs did not support yeast growth on His-deficient SC medium, and only background β-galactosidase activity was expressed (<0.1 Miller units). On the other hand, co-transformation of yeast with BD-IQD20 and AD-CaM/CMLs revealed preferential yet relatively robust interaction of IQD20 with CaM2 (2.2 Miller units) and CML13 (1.2 Miller units), whereas no interaction was observed for BD-IQD20 and the other 11 AD-CaM/CML fusion proteins (Fig. 4). In summary, although yeast two-hybrid assays may not be the ideal system to study or to identify CaM target proteins (9), our results indicate weak but differential interaction of IQD1 and IQD20 with CaM/CMLs *in vivo* and thus support our *in vitro* interaction studies.

IQD1 Interacts with KLCR1—Because *IQD1* is highly expressed in flowers and developing siliques of *A. thaliana* (16),

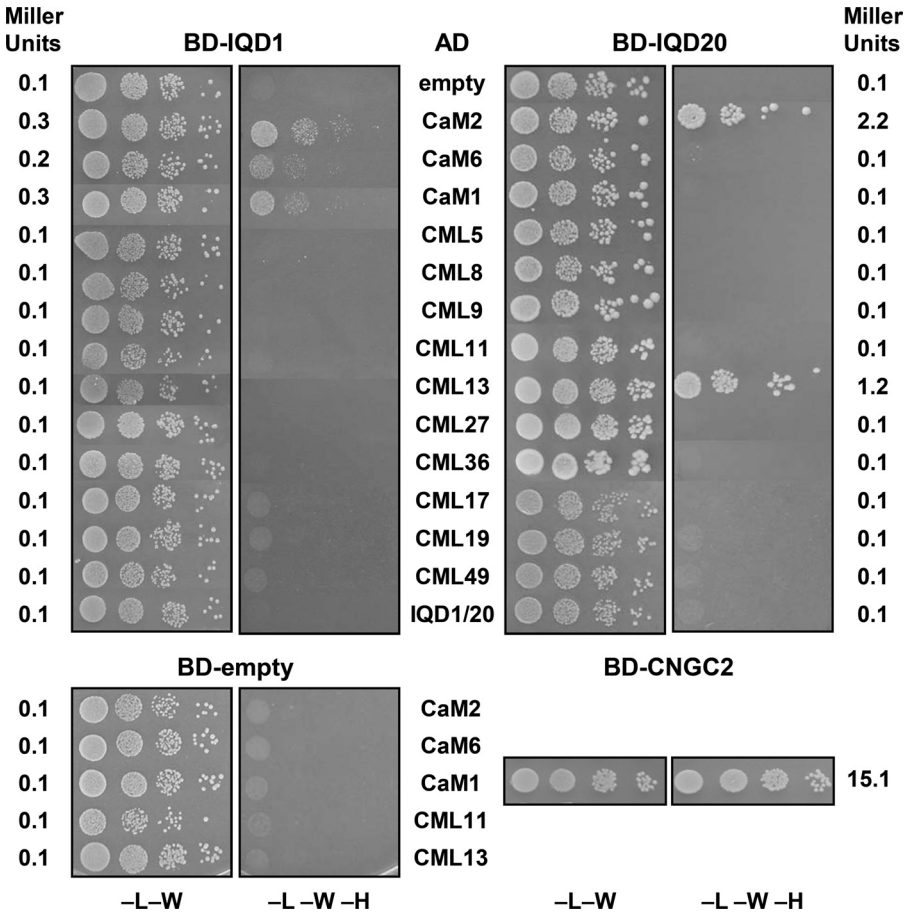

FIGURE 4. **IQD1 and IQD20 interact with *Arabidopsis* CaM/CMLs in the yeast two-hybrid system.** Yeast cells containing the indicated combinations of *IQD1*, *IQD20*, or *CNGC2* cDNAs in the bait Gal4 DNA binding domain vector (*panels BD-IQD1*, *BD-IQD20*, *BD-CNGC2*, and *BD-empty* for control) and different *CaM* or *CML* cDNAs as well as *IQD1* or *IQD20* cDNAs in the prey Gal4 activation domain vector (listed in center AD column) were grown in serial 10-fold dilutions on (−*L*−*W*) SD medium to select for the presence of both vectors and on growth restrictive (−*L*−*W*−*H*) SD medium to test for interaction of the encoded fusion proteins (note, the *upper panels* are composites from different but representative agar plates). The *left* and *right columns* list the corresponding values (Miller units) of quantitative yeast two-hybrid interaction assays (β-galactosidase reporter activity). Qualitative and quantitative interaction assays were repeated 3–5 times giving similar results.

we screened a flower cDNA library for IQD1-interacting proteins. The cDNA library was constructed by recombination with pGADT7-Rec vector in yeast strain AH109, resulting in a fusion of each cDNA with the Gal4AD. Full-length cDNA of IQD1 was cloned in-frame with the Gal4DB (pGBKT7-IQD1) bait vector and introduced into yeast strain Y187. Two-hybrid screens were carried out by mating pGBKT7-IQD1 with the pGADT7-cDNA library. The resulting diploid cells were plated on growth restrictive (−Trp, −Leu, −His, −Ade) SD medium. A total of 25 colonies were selected and tested for *lacZ* expression by measurement of β-galactosidase activity in liquid assays. Only 4 of the 25 yeast strains expressed robust β-galactosidase activity (>1.0 Miller units), which were used for plasmid recovery and sequencing of the prey cDNA insert. Three strains harbored cDNAs predicted to encode a tetratricopeptide repeat domain (TPR12)-containing protein (At4g10840), and the fourth library clone encoded a glutathione *S*-transferase (GST) belonging to the tau (U) class of GSTs (GSTU26; At1g17190). Using the predicted At4g10840 protein as a query, we identified two closely related TPR proteins in *Arabidopsis* (55–60% identity) with similarity to mammalian kinesin light chain (KLC) subunits (20–25% identity) of kinesin motor proteins. The three putative *Arabidopsis* KLCs, encoded by At4g10840, At3g27960, and At1g27500, are hereafter referred to as KLCR proteins, KLCR1-KLCR3 (supplemental Fig. S2). Superimposition of the modeled KLCR1 protein and of the experimentally solved KLC1-TPR or KLC2-TPR domains confirm presence of a structurally similar TPR12-type domain in KLCR1, which suggests functional conservation of human KLC and *Arabidopsis* KLCR proteins (supplemental Fig. S3).

The original diploids expressing BD-IQD1/AD-KLCR1 and BD-IQD1/AD-GSTU26 produced 13.5 ± 1.6 and 9.5 ± 1.3 Miller units of β-galactosidase activity ($n = 5–6$), respectively, which is indicative of a relatively robust protein-protein interaction. We confirmed these interactions by independent plasmid co-transformation of yeast with IQD1 and KLCR1 or IQD1 and GSTU26 vectors of either configuration (Gal4DB or Gal4AD) as well as with control plasmids (BD-CNGC2/AD-CAM1). After mating, the resulting diploid yeast cells expressing IQD1 and KLCR1 or IQD1 and GSTU26 showed vigorous growth and *lacZ* expression on restrictive (−Trp, −Leu, −His, −Ade) SD medium, which was independent of the bait or prey configuration (Fig. 5). Taken together, our results demonstrate strong and reproducible interactions between IQD1 and

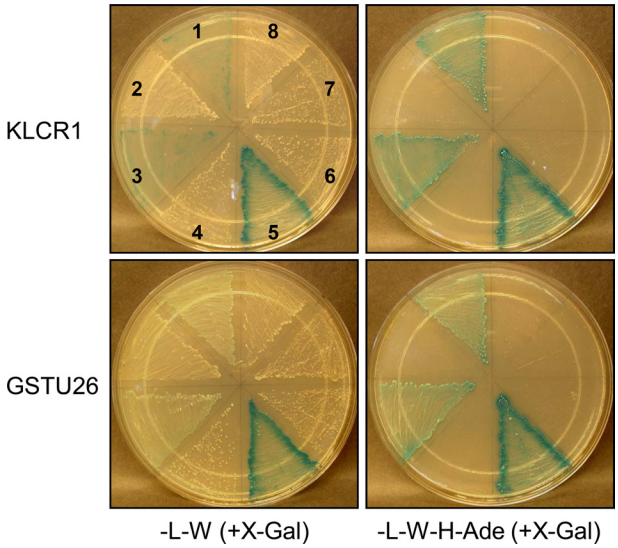

FIGURE 5. **IQD1 interacts with KLCR1 and GSTU26 in the yeast two-hybrid system.** Confirmation of yeast two-hybrid interactions of IQD1 with KLCR1 (*upper panels*) and of IQD1 with GSTU26 (*lower panels*) is shown. Interaction assays between different test and control constructs were performed by co-transformation into yeast cells. Colony growth and *lacZ* expression (+X-gal) was compared on (*−L−W*) SD media to select for bait Gal4-BD and prey Gal4-AD vectors (*left panels*) and on growth restrictive (*−L−W−H−Ade*) SD media to test for protein interaction (*right panels*). Numbers (*1–8*, referring to all plates) indicate the following vector combinations: *1*, BD-KLCR1/AD-IQD1 or BD-GSTU26/AD-IQD1; *2*, BD-KLCR1/AD-empty or BD-GSTU26/AD-empty; *3*, BD-IQD1/AD-KLCR1 or BD-IQD1/AD-GSTU26; *4*, BD-empty/AD-KLCR1 or BD-empty/AD-GSTU26; *5*, BD-CNGC2/AD-CaM1; *6*, BD-empty/AD-KLCR1 or BD-empty/AD-GSTU26; *7*, BD-IQD1/AD-CaM1; *8*, BD-CaM1/AD-IQD1.

KLCR1 as well as between IQD1 and GSTU26, which are comparable with the interaction of the control proteins (CNGC2 and CaM1).

GFP-tagged IQD1 Proteins Localize to Microtubules and the Cell Nucleus—Kinesins are a family of cellular motor proteins that move along polarized microtubule tracks to transport various cargos, which are either directly attached to the KHC or to its associated KLC via the TPR12 domain (34). The putative role of KLCR proteins in microtubular transport and the verified interaction of IQD1 with KLCR1 in yeast prompted us to reinvestigate the subcellular localization of IQD1. We previously reported targeting of an IQD1∼GFP fusion protein to the cell nucleus when expressed under the control of the constitutive *CaMV* 35S promoter in roots of transgenic *Arabidopsis* plants (16). Here, we transiently expressed $35S_{Pro}$::*GFP*, $35S_{Pro}$::*IQD1∼GFP* or $35S_{Pro}$::*GFP∼IQD1* constructs in tobacco leaves (*N. benthamiana*) and monitored GFP fluorescence by confocal laser scanning microscopy at high resolution (Fig. 6). As expected for control transformations, the GFP protein localized to the cytosol and cell nucleus (Fig. 6*A*). For transient expression of C-terminal IQD1∼GFP or N-terminal GFP∼IQD1 fusion proteins, we confirmed nuclear localization of IQD1 but observed additional GFP fluorescence associated with cytoskeletal structures (Fig. 6, *B* and *C*, and supplemental Fig. S4). Because KLCR1 likely interacts with kinesin motor proteins that transport cargo along microtubule tracks, we examined the effect of oryzalin, an herbicide promoting microtubule depolymerization. As shown in Fig. 6*D*, oryzalin treatment caused collapse of cytoskeletal-associated GFP∼IQD1 fluorescence, indicating association of IQD1 with the microtubular network. In addition, we studied oryzalin-dependent GFP∼IQD1 localization in hypocotyl tissues of transgenic *Arabidopsis* seedlings (Fig. 6, *E* and *F*). The results in a stable, homologous plant transformation system are consistent with the observation in transiently transformed tobacco leaves (Fig. 6, compare *panels E* and *F*, with *panels C* and *D*). We independently analyzed the subcellular localization of GFP∼IQD1 in transgenic plants by co-immunolabeling of microtubules (anti-α-tubulin) and GFP∼IQD1 (anti-GFP), which demonstrated co-localization of both proteins to microtubules (Fig. 6, *G–L*).

IQD1 Recruits KLCR1 and CaM2 to Microtubules—Because KLCR1 is predicted to assist kinesins in cargo transport along microtubules, we first compared the subcellular localization of GFP∼IQD1 with RFP∼KLCR1 in tobacco leaves that were transiently transfected with $35S_{Pro}$::*GFP∼IQD1* or $35S_{Pro}$::*RFP∼KLCR1* plasmids. Although GFP∼IQD1 localized to microtubules (Fig. 7, *A–C*), expressed RFP∼KLCR1 displayed diffuse cellular fluorescence, indicative of cytosolic localization (Fig. 7, *D–F*). Interestingly, when both DNA constructs were co-transfected, RFP∼KCLR1 co-localized with the microtubular pattern of GFP∼IQD1 fluorescence (Fig. 7, *G–I*), indicating recruitment of RFP∼KLCR1 to the microtubular network by GFP∼IQD1, most likely via direct interaction *in planta*. Similarly, transient expression of RFP∼CaM2 alone revealed red fluorescence consistent with cytosolic localization of tagged CaM2 (Fig. 7, *J–L*). Again, co-expression of RFP∼CaM2 and GFP∼IQD1 caused microtubular co-localization of both fusion proteins, suggesting IQD1-dependent recruitment of CaM2 to the microtubules (Fig. 7, *M–O*). Additional co-transfection experiments support a role of IQD1 for recruiting KLCR1 and CaM2 to the microtubular skeleton. Although co-expression of GFP∼KLCR1 and RFP∼CaM2 did not alter the cytosolic localization of either protein (Fig. 7, *P–R*), co-expression of both protein fusions together with untagged IQD1 resulted in a microtubular localization of GFP∼KLCR1 and RFP∼CaM2 (Fig. 7, *S–U*). These data also support the functionality of the GFP∼IQD1 protein fusion (Fig. 7, *G–I*, *M–O*, and *S–U*). Taken together, our results demonstrate co-localization of IQD1, KLCR1, and CaM2 to microtubules and further indicate IQD1-dependent recruitment of KLCR1 and CaM2 to the microtubular network via direct interaction.

DISCUSSION

Plant-specific *IQD* gene families, first annotated in *Arabidopsis* and rice, encode a major class of putative CaM targets, with about 30 genes expressed in either plant species (17). Although the biological roles for select IQD proteins are beginning to emerge, their mechanisms of action are elusive (16, 20–22). Here we studied the ability of IQD1 to bind to various *Arabidopsis* CaM/CMLs, mapped its CaM-recruitment domain, and searched for IQD1 interactors to gain first insight into its biochemical function. We used pulldown assays to probe the interaction with two canonical CaMs and two CMLs from *Arabidopsis*. This study revealed Ca^{2+}-dependent recruitment of all tested CaM/CMLs by IQD1, demonstrating its potential to interact with divergent CaM/CML sensors (Fig. 1). We verified binding of IQD1 to CaM2 by gel overlay assays. In contrast to pulldown assays, we observed interaction in the

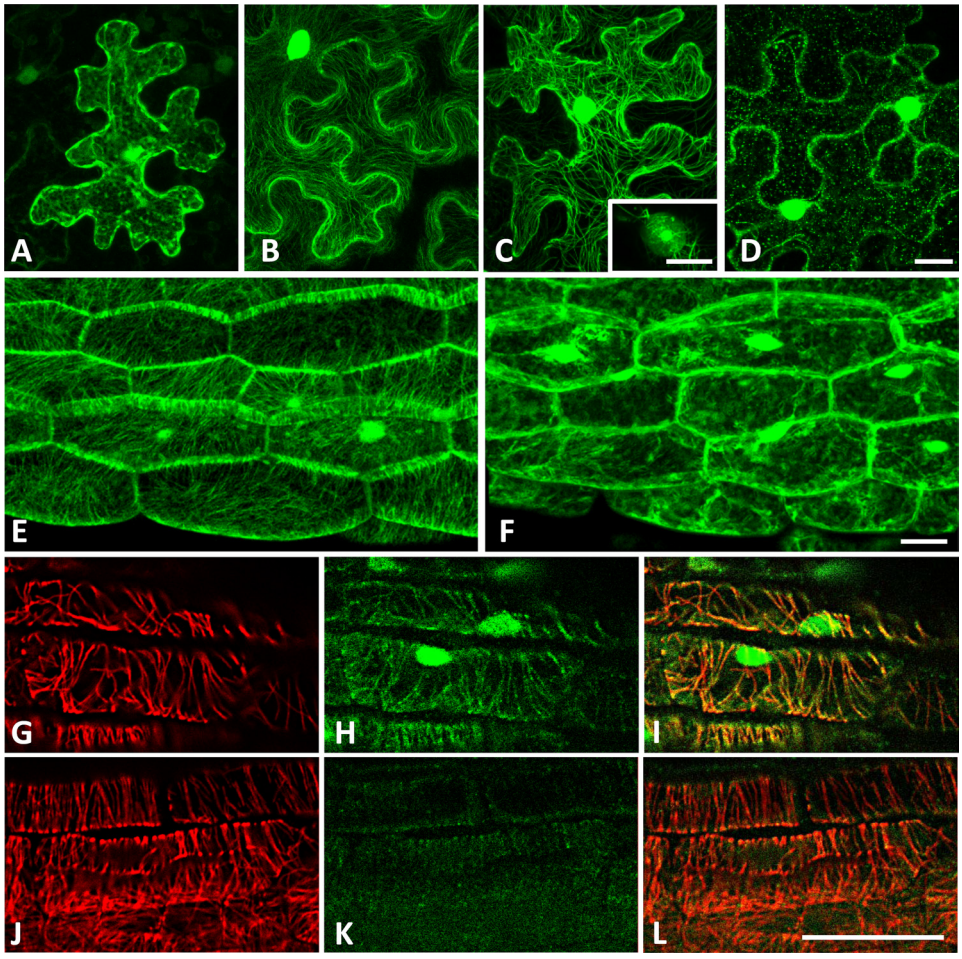

FIGURE 6. **GFP-tagged IQD1 proteins localize to microtubules and the cell nucleus.** *A–D*, tobacco leaves (*N. benthamiana*) were transiently transfected with *Agrobacterium* strains harboring plasmids supporting expression of *CaMV 35S*$_{Pro}$*::GFP* (*A*), *CaMV 35S*$_{Pro}$*::IQD1∼GFP* (*B*), and *CaMV 35S*$_{Pro}$*::GFP∼IQD1* (*C* and *D*). Samples were collected 2 days after infiltration and visualized by confocal laser scanning microscopy after mock treatment with DMSO (*A–C*) or after infiltration with 50 μM oryzalin for 90 min (*D*). *E* and *F*, transgenic *Arabidopsis* seedlings (*CaMV 35S*$_{Pro}$*::GFP∼IQD1*) were visualized (three-dimensional projections) before (*E*) or after (*F*) treatment with 5 μM oryzalin for 60 min. *G–L*, GFP∼IQD1 and microtubules were co-immunolabeled in transgenic (*G–I*) and wild type (*J–L*) *Arabidopsis* seedlings using a combination of a rat anti-α tubulin antibody (*G* and *J*) and a green fluorescent monoclonal mouse anti-GFP antibody (*H* and *K*). Merged images are shown (*I* and *L*). *Scale bars*, 20 μm. Nuclear localization of GFP-tagged IQD1 was additionally demonstrated by DAPI (4′,6′ diamino-2-phenylindole·2HCl) staining (see supplemental Fig. S4).

absence of Ca^{2+} (supplemental Fig. S1, Fig. 2). Using similar overlay assays, CaM interaction in the absence but not the presence of Ca^{2+} was reported for OsCBT, a putative CaM binding transcription factor from rice (31), or for AtBAG6, a novel *Arabidopsis* CaM-binding protein (32). Deletion analysis of both proteins demonstrated a role of canonical IQ motifs for mediating their interaction with Ca^{2+}-free CaM (31, 32). Typically, proteins containing complete canonical IQ motifs but no other CaM interaction motifs do not require Ca^{2+} for CaM binding, such as myosin (35), whereas proteins having incomplete IQ-like motifs tend to bind to Ca^{2+}-CaM with higher affinity than to apoCaM (36–38). Deletion mapping of IQD1 confirmed the importance of the IQ67 domain for CaM interaction (Fig. 2), which contains one complete and one incomplete IQ consensus as well as three interspersed 1-5-10 motifs (16), suggesting complex and differential interaction of IQD1 with both apo- and Ca^{2+}-CaM/CML sensors. It is likely that the physicochemical conditions during pulldown assays (native IQD1 in solution) and gel overlay assays (membrane-immobilized, renatured IQD1) differentially favor the accessibility of Ca^{2+}-dependent or Ca^{2+}-independent CaM binding motifs. Whereas high affinity binding (K_d values in the nM range) is typical for Ca^{2+}-CaM binding proteins (39–41), the relatively low affinity of IQD1 for apoCaM2 (K_d∼ 0.6 μM) in gel overlay assays (Fig. 3) is consistent with Ca^{2+}-independent CaM interactions reported for proteins binding to apoCaM, *e.g.* neuromodulin (K_d ∼ 1 μM) (13, 42). Our results of two unrelated CaM interaction assays validate the presence of functional Ca^{2+}-independent and Ca^{2+}-dependent CaM recruitment motifs in the IQ67 domain. Its importance for mediating CaM interaction is further supported by experiments with IQD20, which comprises only a short N-terminal extension in addition to the IQ67 domain but binds to bovine CaM (17) and *Arabidopsis* CaM2 (supplemental Fig. S1) in pulldown and gel overlay assays, respectively.

The capacity of IQD proteins to recruit CaM is further demonstrated by yeast two-hybrid assays (Fig. 4). These reveal weak but differential interaction of IQD1 and IQD20 with only a few of the 13 CaM/CMLs tested, suggesting regulation of IQD function by specific CaM/CML sensors. Interrogation of a recently

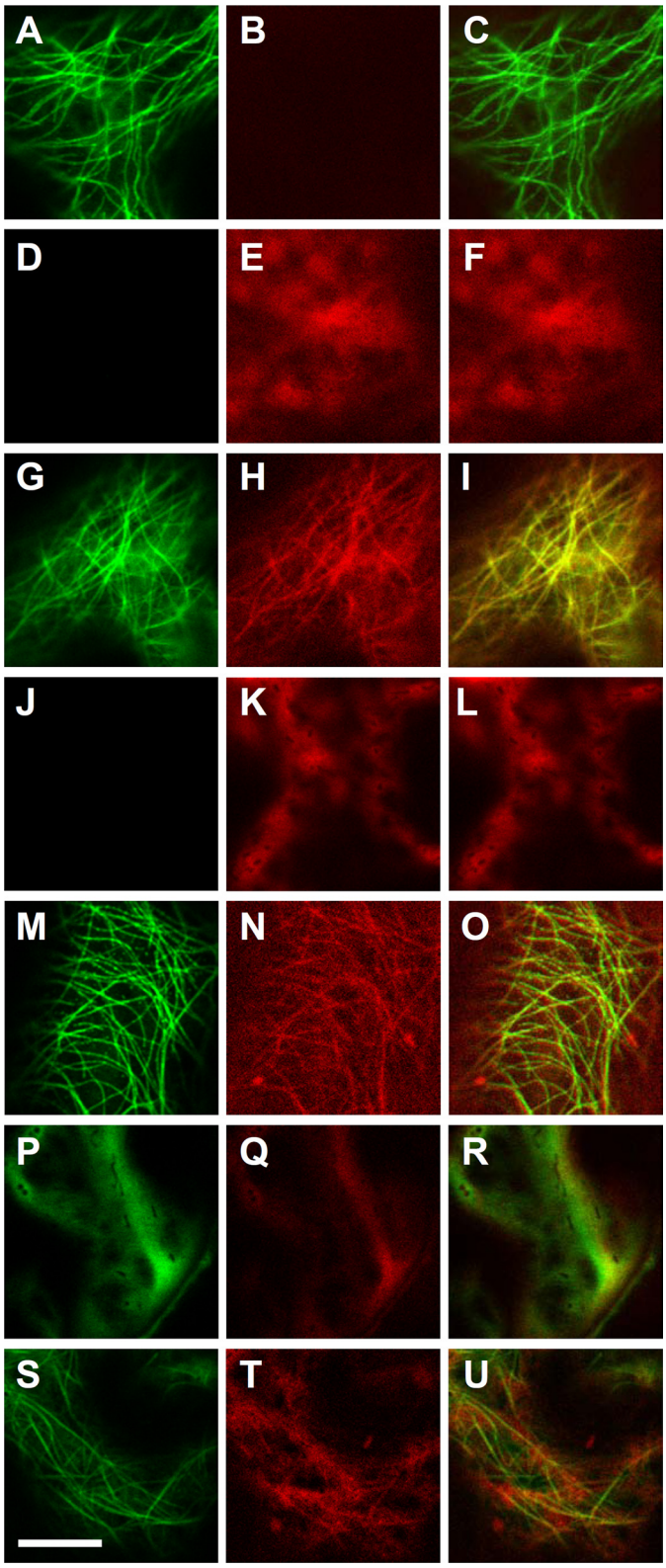

FIGURE 7. **IQD1 recruits KLCR1 and CaM2 to microtubules.** Tobacco leaves (*N. benthamiana*) were (co)infiltrated with *Agrobacterium* strains harboring plasmids supporting *CaMV* 35S promoter-driven expression of GFP∼IQD1 alone (*A–C*), mRFP∼KLCR1alone (*D–F*), GFP∼IQD1 and mRFP∼KLCR1 (*G–I*), mRFP∼CaM2 alone (*J–L*), GFP∼IQD1 and mRFP∼CaM2 (*M–O*), and GFP ∼KLCR1 and mRFP∼CaM2 (*P–R*) as well as of untagged IQD1 together with GFP∼KLCR1 and mRFP∼CaM2 (*S–U*). Panels of the *left column* show the GFP signal, panels of the *center column* the RFP signal, and panels of the *right column* the merged GFP and RFP signals. Images were obtained on a *Zeiss LSM700* confocal laser scanning microscope using sequential mode for clear separation of GFP and RFP signals. *Scale bar*, 10 μm. Transfection experiments were repeated at least three times with different sets of tobacco plants. Representative images of transfected leaf epidermal cells are shown.

published *Arabidopsis* interactome map retrieved evidence for the interaction of IQD1, IQD23, and IQD31 with CaM1 as well as of IQD31 with CML13 in yeast (43). Although the yeast system is a widely used approach to study protein interactions *in vivo*, the yeast system is not necessarily a suitable method for characterizing Ca^{2+}-regulated CaM/CML-target interactions due to its difficulties to control Ca^{2+} concentration (9). Nonetheless, we performed yeast two-hybrid screens with IQD1 to select *Arabidopsis* CaM/CMLs and novel interactors. Although we did not recover any of the Ca^{2+} sensors, we repeatedly isolated cDNAs encoding KLCR1 and GSTU26, and we confirmed the interaction with IQD1 (Fig. 5). GSTU26 belongs to the plant-specific tau (U) class of GST enzymes of undefined metabolic functions (44–46); however, GSTUs were shown to selectively retain *S*-acyl-glutathione adducts, possibly to protect their unstable products upon formation *in vivo* (47). Interestingly, GSTU26 is closely related to GSTU20 (44). The latter was implicated in the conjugation of glutathione with activated aliphatic aldoximes to form structurally analogous *S*-hydroxamyl-glutathione adducts during glucosinolate biosynthesis (48). The expression of *GSTU26* differentially responds to challenge with plant pathogens and treatment with defense-related hormones, jasmonic and salicylic acid (49). Thus, GSTU26 and IQD1 may both play a role for the production and regulation of glucosinolate phytoanticipins in plant defense (16).

The IQD1-KLCR1 interaction in yeast (Fig. 5) is supported by querying the *Arabidopsis* interactome database, which points to interactions between IQD and KLCR protein, *i.e.* IQD2 with At4g10840 (KLCR1) and At3g27960 (KLCR2) and IQD23 with At3g27960 (KLCR2) (43). The *Arabidopsis* KLCRs are similar to human KLCs (supplemental Figs. S2 and S3) and may be functionally equivalent in recruiting various cargos to KHCs. Kinesins are a class of microtubule-associated motor proteins that function in cell division and facilitate directional transport of organelles, vesicles, protein complexes, and mRNA-protein particles to specific destinations, generally toward the cell periphery (34, 50, 51). The cargo is either directly attached to the globular C-terminal tail of the KHC homodimer or indirectly via associated KLCs or via KLC binding adaptors that provide a scaffold for additional protein interactions. The KLC subunit contains an N-terminal heptad repeat region for binding to the coiled-coil stalk of the KHC dimer followed by several TPR motifs and a variable C-terminal domain that typically recognizes the C terminus of their partner scaffold protein. Mounting evidence in animals on kinesin-cargo interactions indicates that KLC-interacting scaffolds regulate cargo recruitment and kinesin activation by relieving autoinhibition. Even entire preassembled signaling modules such as mitogen-activated protein kinase cascades associated with vesicle-bound transmembrane receptors are tethered to KHC-KLC tetramers via scaffold proteins, which trigger and inform transport along microtubules to their final membrane destination. The assembly, loading, and unloading of scaffold-

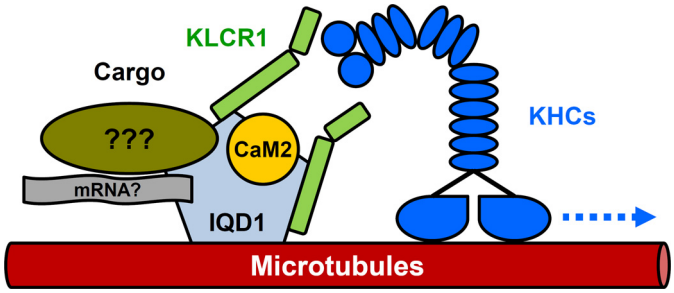

FIGURE 8. **Working model of IQD1.** The IQD1 protein localizes to the cell nucleus and microtubules and interacts with KLCR1and CaM/CML Ca^{2+} sensors such as CaM2. IQD1 is proposed to function as a scaffold protein that likely recruits in a Ca^{2+}-CaM-regulated manner various cargos to kinesins (KHCs) via associated KLCR1 for unidirectional transport along microtubule tracks. Transport cargos are currently unknown and may include ribonucleoprotein complexes.

associated cargo complexes are tightly controlled by phosphorylation, GTPase activity, and Ca^{2+}-signaling (50–52). Thus, scaffold proteins serve as critical nodes that integrate multiple signaling pathways to coordinate diverse cellular activities (53, 54).

Although mammalian KHC and KLC subunits are encoded by 45 and 4 genes, respectively, the *Arabidopsis* kinesin family comprises 61 predicted members (34, 55, 56). The precise functions and biological roles for about two-thirds of *Arabidopsis* kinesins are not understood, and nothing is known about their associated light chains (55). Cargo selection, regulation of motor activity, and associated biological processes remain unexplored in plants, with the notable exception of a kinesin-like CaM-binding protein involved in the regulation of cell division and trichome morphogenesis (55, 57). Our study uncovers a novel link between Ca^{2+} signaling and the regulation of kinesin motor activity via direct interactions of CaM/CML, IQD, and KLRC proteins. This proposition is supported by the subcellular localization of IQD1 to microtubules (Fig. 6), a feature shared by most members of the *Arabidopsis* IQD family.[8] Our co-transfection studies in tobacco further indicate recruitment of KLCR1 as well as CaM2 to the microtubules via IQD1 (Fig. 7). The prospect arises that IQD proteins provide an assortment of KLCR-interacting scaffolds for various kinesin-dependent transport processes (see Fig. 8). Given the affinity of IQD1 for artificial single-stranded nucleic acid substrates (supplemental Fig. S5), IQD-facilitated transport along microtubules may comprise translocation of RNA-protein complexes to distinct cellular compartments, which is an important mechanism for coupling gene expression with efficient protein sorting (58, 59).

We obtained first insight into the biochemical functions of IQD1, likely having implications for other IQD proteins, but are left to speculate on the role of IQD1 in glucosinolate metabolism and plant defense. *IQD1* is mainly expressed in the vascular bundles, a pattern characteristic of numerous glucosinolate-related genes, and its overexpression stimulates glucosinolate production and defense responses (16). In *Arabidopsis*, glucosinolates accumulate to very high concentrations (>130 mM) in the sulfur-rich S-cells, which surround the phloem zone of vascular bundles and expand to a length of >1 mm (60). Because S-cells are thought to sustain glucosinolate synthesis (60), the highly polarized cells likely necessitate active translocation of metabolons or RNA-protein complexes. Likewise, intracellular transport processes such as vesicle trafficking are crucial for the rapid deployment of defensive layers of callose at the site of pathogen contact. Interestingly, pathogen perception activates turnover of specific glucosinolates, which is necessary for triggering biosynthesis of callose and its site-specific deposition (61, 62). In conclusion, our study provides a first molecular framework for dissecting the biochemical functions of IQD1 and related proteins in *A. thaliana* and other plant species.

Acknowledgments—We thank Claudia Köhler (Swedish University of Agricultural Sciences, Uppsala) for CaM/CML plasmids, Petra Dietrich und Cornelia Fischer (University of Erlangen-Nürnberg) for the CaM2-pENTR/ D-TOPO vector, Kristin Eismann for technical assistance, and Claus Wasternack for critical reading of the manuscript.

[8] K. Bürstenbinder and S. Abel, unpublished work.

REFERENCES

1. Dodd, A. N., Kudla, J., and Sanders, D. (2010) The language of calcium signaling. *Annu. Rev. Plant Biol.* **61,** 593–620
2. DeFalco, T. A., Bender, K. W., and Snedden, W. A. (2010) Breaking the code. Ca^{2+} sensors in plant signalling. *Biochem. J.* **425,** 27–40
3. Reddy, A. S., Ali, G. S., Celesnik, H., and Day, I. S. (2011) Coping with stresses. Roles of calcium- and calcium/calmodulin-regulated gene expression. *Plant Cell* **23,** 2010–2032
4. Day, I. S., Reddy, V. S., Shad Ali, G., and Reddy, A. S. (2002) Analysis of EF-hand-containing proteins in *Arabidopsis*. *Genome Biol* **3,** RESEARCH0056
5. Sanders, D., Pelloux, J., Brownlee, C., and Harper, J. F. (2002) Calcium at the crossroads of signaling. *Plant Cell* **14,** S401–S417
6. Hrabak, E. M., Chan, C. W., Gribskov, M., Harper, J. F., Choi, J. H., Halford, N., Kudla, J., Luan, S., Nimmo, H. G., Sussman, M. R., Thomas, M., Walker-Simmons, K., Zhu, J. K., and Harmon, A. C. (2003) The *Arabidopsis* CDPK-SnRK superfamily of protein kinases. *Plant Physiol* **132,** 666–680
7. Weinl, S., and Kudla, J. (2009) The CBL-CIPK Ca^{2+}-decoding signaling network. Function and perspectives. *New Phytol.* **184,** 517–528
8. Luan, S. (2009) The CBL-CIPK network in plant calcium signaling. *Trends Plant Sci.* **14,** 37–42
9. Reddy, A. S., Ben-Hur, A., and Day, I. S. (2011) Experimental and computational approaches for the study of calmodulin interactions. *Phytochemistry* **72,** 1007–1019
10. McCormack, E., Tsai, Y. C., and Braam, J. (2005) Handling calcium signaling. *Arabidopsis* CaMs and CMLs. *Trends Plant Sci.* **10,** 383–389
11. Reddy, V. S., and Reddy, A. S. (2004) Proteomics of calcium-signaling components in plants. *Phytochemistry* **65,** 1745–1776
12. Bouché, N., Yellin, A., Snedden, W. A., and Fromm, H. (2005) Plant-specific calmodulin-binding proteins. *Annu. Rev. Plant Biol.* **56,** 435–466
13. Rhoads, A. R., and Friedberg, F. (1997) Sequence motifs for calmodulin recognition. *FASEB J.* **11,** 331–340
14. Bähler, M., and Rhoads, A. (2002) Calmodulin signaling via the IQ motif. *FEBS Lett.* **513,** 107–113
15. Hoeflich, K. P., and Ikura, M. (2002) Calmodulin in action. Diversity in target recognition and activation mechanisms. *Cell* **108,** 739–742
16. Levy, M., Wang, Q., Kaspi, R., Parrella, M. P., and Abel, S. (2005) *Arabidopsis* IQD1, a novel calmodulin-binding nuclear protein, stimulates glucosinolate accumulation and plant defense. *Plant J.* **43,** 79–96
17. Abel, S., Savchenko, T., and Levy, M. (2005) Genome-wide comparative analysis of the IQD gene families in *Arabidopsis thaliana* and *Oryza sativa*. *BMC Evol Biol* **5,** 72
18. Grubb, C. D., and Abel, S. (2006) Glucosinolate metabolism and its control. *Trends Plant Sci.* **11,** 89–100

19. Halkier, B. A., and Gershenzon, J. (2006) Biology and biochemistry of glucosinolates. *Annu. Rev. Plant Biol.* **57,** 303–333
20. Zentella, R., Zhang, Z. L., Park, M., Thomas, S. G., Endo, A., Murase, K., Fleet, C. M., Jikumaru, Y., Nambara, E., Kamiya, Y., and Sun, T. P. (2007) Global analysis of della direct targets in early gibberellin signaling in *Arabidopsis*. *Plant Cell* **19,** 3037–3057
21. Xiao, H., Jiang, N., Schaffner, E., Stockinger, E. J., and van der Knaap, E. (2008) A retrotransposon-mediated gene duplication underlies morphological variation of tomato fruit. *Science* **319,** 1527–1530
22. Wu, S., Xiao, H., Cabrera, A., Meulia, T., and van der Knaap, E. (2011) SUN regulates vegetative and reproductive organ shape by changing cell division patterns. *Plant Physiol.* **157,** 1175–1186
23. Köhler, C., and Neuhaus, G. (2000) Characterisation of calmodulin binding to cyclic nucleotide-gated ion channels from *Arabidopsis thaliana*. *FEBS Lett.* **471,** 133–136
24. Laemmli, U. K. (1970) Cleavage of structural proteins during the assembly of the head of bacteriophage T4. *Nature* **227,** 680–685
25. Kim, J., Harter, K., and Theologis, A. (1997) Protein-protein interactions among the Aux/IAA proteins. *Proc. Natl. Acad. Sci. U.S.A.* **94,** 11786–11791
26. Karimi, M., Inzé, D., and Depicker, A. (2002) GATEWAY vectors for *Agrobacterium*-mediated plant transformation. *Trends Plant Sci.* **7,** 193–195
27. Nakagawa, T., Suzuki, T., Murata, S., Nakamura, S., Hino, T., Maeo, K., Tabata, R., Kawai, T., Tanaka, K., Niwa, Y., Watanabe, Y., Nakamura, K., Kimura, T., and Ishiguro, S. (2007) Improved Gateway binary vectors. High performance vectors for creation of fusion constructs in transgenic analysis of plants. *Biosci. Biotechnol. Biochem.* **71,** 2095–2100
28. Voinnet, O., Rivas, S., Mestre, P., and Baulcombe, D. (2003) An enhanced transient expression system in plants based on suppression of gene silencing by the p19 protein of tomato bushy stunt virus. *Plant J* **33,** 949–956
29. Clough, S. J. (2005) Floral dip, *Agrobacterium*-mediated germ line transformation. *Methods Mol. Biol.* **286,** 91–102
30. Müller, J., Beck, M., Mettbach, U., Komis, G., Hause, G., Menzel, D., and Samaj, J. (2010) *Arabidopsis* MPK6 is involved in cell division plane control during early root development and localizes to the pre-prophase band, phragmoplast, trans-Golgi network, and plasma membrane. *Plant J* **61,** 234–248
31. Choi, M. S., Kim, M. C., Yoo, J. H., Moon, B. C., Koo, S. C., Park, B. O., Lee, J. H., Koo, Y. D., Han, H. J., Lee, S. Y., Chung, W. S., Lim, C. O., and Cho, M. J. (2005) Isolation of a calmodulin-binding transcription factor from rice (*Oryza sativa* L.). *J. Biol. Chem.* **280,** 40820–40831
32. Kang, C. H., Jung, W. Y., Kang, Y. H., Kim, J. Y., Kim, D. G., Jeong, J. C., Baek, D. W., Jin, J. B., Lee, J. Y., Kim, M. O., Chung, W. S., Mengiste, T., Koiwa, H., Kwak, S. S., Bahk, J. D., Lee, S. Y., Nam, J. S., Yun, D. J., and Cho, M. J. (2006) AtBAG6, a novel calmodulin-binding protein, induces programmed cell death in yeast and plants. *Cell Death Differ.* **13,** 84–95
33. McCormack, E., and Braam, J. (2003) Calmodulin and related potential calcium sensors of *Arabidopsis*. *New Phytol.* **159,** 585–598
34. Verhey, K. J., Kaul, N., and Soppina, V. (2011) Kinesin assembly and movement in cells. *Annu. Rev. Biophys.* **40,** 267–288
35. Houdusse, A., Gaucher, J. F., Krementsova, E., Mui, S., Trybus, K. M., and Cohen, C. (2006) Crystal structure of apocalmodulin bound to the first two IQ motifs of myosin V reveals essential recognition features. *Proc. Natl. Acad. Sci. U.S.A.* **103,** 19326–19331
36. Houdusse, A., and Cohen, C. (1995) Target sequence recognition by the calmodulin superfamily. Implications from light chain binding to the regulatory domain of scallop myosin. *Proc. Natl. Acad. Sci. U.S.A.* **92,** 10644–10647
37. Munshi, H. G., Burks, D. J., Joyal, J. L., White, M. F., and Sacks, D. B. (1996) Ca^{2+} regulates calmodulin binding to IQ motifs in IRS-1. *Biochemistry* **35,** 15883–15889
38. DeFalco, T. A., Chiasson, D., Munro, K., Kaiser, B. N., and Snedden, W. A. (2010) Characterization of GmCaMK1, a member of a soybean calmodulin-binding receptor-like kinase family. *FEBS Lett.* **584,** 4717–4724
39. Bouché, N., Scharlat, A., Snedden, W., Bouchez, D., and Fromm, H. (2002) A novel family of calmodulin binding transcription activators in multicellular organisms. *J. Biol. Chem.* **277,** 21851–21861
40. Yang, T., and Poovaiah, B. W. (2000) An early ethylene up-regulated gene encoding a calmodulin-binding protein involved in plant senescence and death. *J. Biol. Chem.* **275,** 38467–38473
41. Reddy, V. S., Safadi, F., Zielinski, R. E., and Reddy, A. S. (1999) Interaction of a kinesin-like protein with calmodulin isoforms from *Arabidopsis*. *J. Biol. Chem.* **274,** 31727–31733
42. Black, D. J., LaMartina, D., and Persechini, A. (2009) The IQ domains in neuromodulin and PEP19 represent two major functional classes. *Biochemistry* **48,** 11766–11772
43. Arabidopsis Interactome Mapping Consortium (2011) Evidence for network evolution in an *Arabidopsis* interactome map. *Science* **333,** 601–607
44. Dixon, D. P., Lapthorn, A., and Edwards, R. (2002) Plant glutathione transferases. *Genome Biol.* **3,** REVIEWS3004
45. Wagner, U., Edwards, R., Dixon, D. P., and Mauch, F. (2002) Probing the diversity of the *Arabidopsis* glutathione *S*-transferase gene family. *Plant Mol. Biol.* **49,** 515–532
46. Dixon, D. P., Skipsey, M., and Edwards, R. (2010) Roles for glutathione transferases in plant secondary metabolism. *Phytochemistry* **71,** 338–350
47. Dixon, D. P., and Edwards, R. (2009) Selective binding of glutathione conjugates of fatty acid derivatives by plant glutathione transferases. *J. Biol. Chem.* **284,** 21249–21256
48. Sønderby, I. E., Geu-Flores, F., and Halkier, B. A. (2010) Biosynthesis of glucosinolates. Gene discovery and beyond. *Trends Plant Sci.* **15,** 283–290
49. Nutricati, E., Miceli, A., Blando, F., and De Bellis, L. (2006) Characterization of two *Arabidopsis thaliana* glutathione *S*-transferases. *Plant Cell Rep.* **25,** 997–1005
50. Akhmanova, A., and Hammer, J. A., 3rd. (2010) Linking molecular motors to membrane cargo. *Curr. Opin. Cell Biol.* **22,** 479–487
51. Hirokawa, N., Noda, Y., Tanaka, Y., and Niwa, S. (2009) Kinesin superfamily motor proteins and intracellular transport. *Nat. Rev. Mol. Cell Biol.* **10,** 682–696
52. Schnapp, B. J. (2003) Trafficking of signaling modules by kinesin motors. *J. Cell Sci.* **116,** 2125–2135
53. Brown, M. D., and Sacks, D. B. (2009) Protein scaffolds in MAP kinase signalling. *Cell Signal* **21,** 462–469
54. White, C. D., Brown, M. D., and Sacks, D. B. (2009) IQGAPs in cancer. A family of scaffold proteins underlying tumorigenesis. *FEBS Lett.* **583,** 1817–1824
55. Zhu, C., and Dixit, R. (2012) Functions of the *Arabidopsis* kinesin superfamily of microtubule-based motor proteins. *Protoplasma* **249,** 887–899
56. Reddy, A. S., and Day, I. S. (2001) Kinesins in the *Arabidopsis* genome. A comparative analysis among eukaryotes. *BMC Genomics* **2,** 2
57. Reddy, V. S., Day, I. S., Thomas, T., and Reddy, A. S. (2004) KIC, a novel Ca^{2+} binding protein with one EF-hand motif, interacts with a microtubule motor protein and regulates trichome morphogenesis. *Plant Cell* **16,** 185–200
58. Kanai, Y., Dohmae, N., and Hirokawa, N. (2004) Kinesin transports RNA. Isolation and characterization of an RNA-transporting granule. *Neuron* **43,** 513–525
59. Kindler, S., Wang, H., Richter, D., and Tiedge, H. (2005) RNA transport and local control of translation. *Annu. Rev. Cell Dev. Biol.* **21,** 223–245
60. Koroleva, O. A., Gibson, T. M., Cramer, R., and Stain, C. (2010) Glucosinolate-accumulating S-cells in *Arabidopsis* leaves and flower stalks undergo programmed cell death at early stages of differentiation. *Plant J* **64,** 456–469
61. Clay, N. K., Adio, A. M., Denoux, C., Jander, G., and Ausubel, F. M. (2009) Glucosinolate metabolites required for an *Arabidopsis* innate immune response. *Science* **323,** 95–101
62. Bednarek, P., Pislewska-Bednarek, M., Svatos, A., Schneider, B., Doubsky, J., Mansurova, M., Humphry, M., Consonni, C., Panstruga, R., Sanchez-Vallet, A., Molina, A., and Schulze-Lefert, P. (2009) A glucosinolate metabolism pathway in living plant cells mediates broad-spectrum antifungal defense. *Science* **323,** 101–106